Journal of Environment and Earth Science
ISSN 2224-3216 (Paper) ISSN 2225-0948 (Online)
Vol.11, No.16, 2021

Spatial Analysis of Climate variability and Change in the Great Ethiopian Rift Valley Basins

Fitih Ademe*
Melkassa Agricultural Research Center, P.O.Box 436, Adama, Ethiopia

Melat Eshetu
Melkassa Agricultural Research Center, P.O.Box 436, Adama, Ethiopia

Abstract
The generally high temporal and spatial climate variability and change in most parts of Ethiopia, where rainfed farming is the main form of crop production, has been the main cause of food insecurity in significant areas of the country. Spatial variations in selected climate variables were investigated for the great Rift Valley regions of Ethiopia during the baseline (1981-2010) and projected (2021-2100) periods. Baseline climate data from 16 stations that represent different agroecology were obtained from National Meteorology Agency of Ethiopia (NMA) (http://www.ethiomet.gov.et). Corresponding projected data grided over 0.5° X 0.5° were retrieved from eight GCM-RCM combinations under two Representative concentration pathways (RCPs) from CORDEX database (http://www.cordex.org). First order Markov chain model was used for missing rainfall data filling. Coefficient of variation and standardized anomaly index descriptors were used in the analysis of climate data for each station. Spatial maps were then generated from station values using the ordinary kriging method of interpolation. The result indicated that rainfall of the study basins showed both spatial and temporal variabilities. The total annual rainfall showed variation in the year-to-year variability ranging from low in the southern half to high in the northern half of the basins. Seasonal rainfall showed high to very high variability which is challenging to rainfed agriculture. For the projected periods, majority of the climate models projected a decline in annual rainfall and increase in temperature. HadGEM2-ES_RCA4 model simulation suggested precipitation change varying from +4.2 to -16% and +3.8 to -18% for near period under RCP4.5 and RCP8.5 emission scenarios, respectively. Mean temperature is projected to rise from +0.7 to +1.25 ºC under RCP4.5 to +0.9 to +1.6 ºC under RCP8.5 across the GRVB in the near future and further warming was projected in the mid and end centuries. Rainfed crop production in the region, which is already impacted by the current climate variability, is likely to be further challenged with future climate change. As a consequence, specific impact -based adaptation strategies are essential to reduce the vulnerability of rainfed crop production in the area.
Keywords: Climate models, growing season, Rift Valley, seasonal water deficit, dry spell
DOI: 10.7176/JEES/11-16-01
Publication date: June 30th 2021

1. Introduction

Various global and regional studies indicated that climate change is expected to negatively affect crop productivity in most parts of the world, particularly in sub-Saharan Africa (Müller et al., 2011; Thornton et al., 2011). The effect is highly pronounced through the pressure climate change exert on green water resources. The Sub-Saharan Africa, such as Ethiopia is among the most vulnerable regions to climate changes due to its strong dependence on climate sensitive sectors, particularly agriculture (Conway and Schipper, 2011). Past studies revealed that agricultural systems in the developing countries are inherently vulnerable to climate variability (Müller et al., 2011) and climate change is expected to increase this vulnerability (Thornton et al., 2010).

Ethiopia is an agrarian country with majority of the population engaged in this sector. Recent estimates show that agriculture accounts for about 37 percent of GDP, contributes over 70 percent of the export earnings and employs 73 percent of the labor force (UNDP, 2018). The sector however is dominated by subsistence farming, whereby more than 95% is rain-fed (Awulachew et al., 2010) and prone to climatic shocks (Araya and Stroosnijder, 2011). The dependence of the sector on climate is threatening to its overall performance of Ethiopian economy, which is reflected by the existing high correlation between rainfall and GDP fluctuations (World Bank, 2006). Studies indicated that the future climate change may highly likely increase the climate variability and the frequency and magnitude of extreme events (Stern, 2007). Even though the impact of climate change is vast, the changing pattern of precipitation coupled with increased temperature deserves urgent and systematic attention, as it directly affects food security and overall economy in the country.

The biophysical characteristics within Ethiopia are highly varied. The terrain spans from the hot arid desert of the Danakil lowland to the mountainous ranges of the Simien. Overlaid on this terrain, agriculture and land-use activities are extremely diverse. This reflects the variation in climate, soil type and cultural practices across the country. This variation complicates policy planning, particularly since responses to build resilience must be grounded in local contexts (ECRGE, 2015). Clearly understanding the spatial and temporal variability of key

climate variables with respect to differences in agroecology is crucial for the study basins agricultural planning (Segele & Lamb 2005). These would help to optimize the use of available rainfall with respect to meeting crop water requirements. The studies conducted so far in Ethiopia, however, did not consider spatial variations in the potential impacts of climate change in such contrasting agroecology of the country.

The study gave adequate attention to rain-fed agriculture as a key element in food security in Ethiopia (NMA 1996). Given the relative contribution of *Kiremt* to the national crop production and its relative stability in rainfall variability as compared to the *Bulg* season (NMA, 1996), understanding the spatial variability and change of *Kiremt* season will be very crucial and sensible. Hence, this study presents the spatial variability of the most crucial agroclimatic variables and their corresponding changes in time, with due emphasis on agroecological variations over the great Rift Valley regions of Ethiopia during the main growing season.

2. Materials and Methods

2.1 Study area description

The Ethiopian Rift Valley comprise three river basins (Awash, Omo-Gibe and Rift Valley Lakes basins) and a dry basin (Danakil basin, omitted in this study due to its insignificant agricultural contribution) (MoWE, 2010). The study region (hereafter referred to Great Rift Valley Basins, GRVB) extends from the northeastern Awash basin to southwestern edges of Rift Valley Lakes and Omo-Gibe basins. The area is situated roughly between 4.5^0 - 12^0 N latitude and 36^0 – 44 ^{0}E longitude with an estimated total area of 243,640 square kilometers (ARBWA, 2013), which is nearly 21.4% of the total land area of the country (Fig 1).

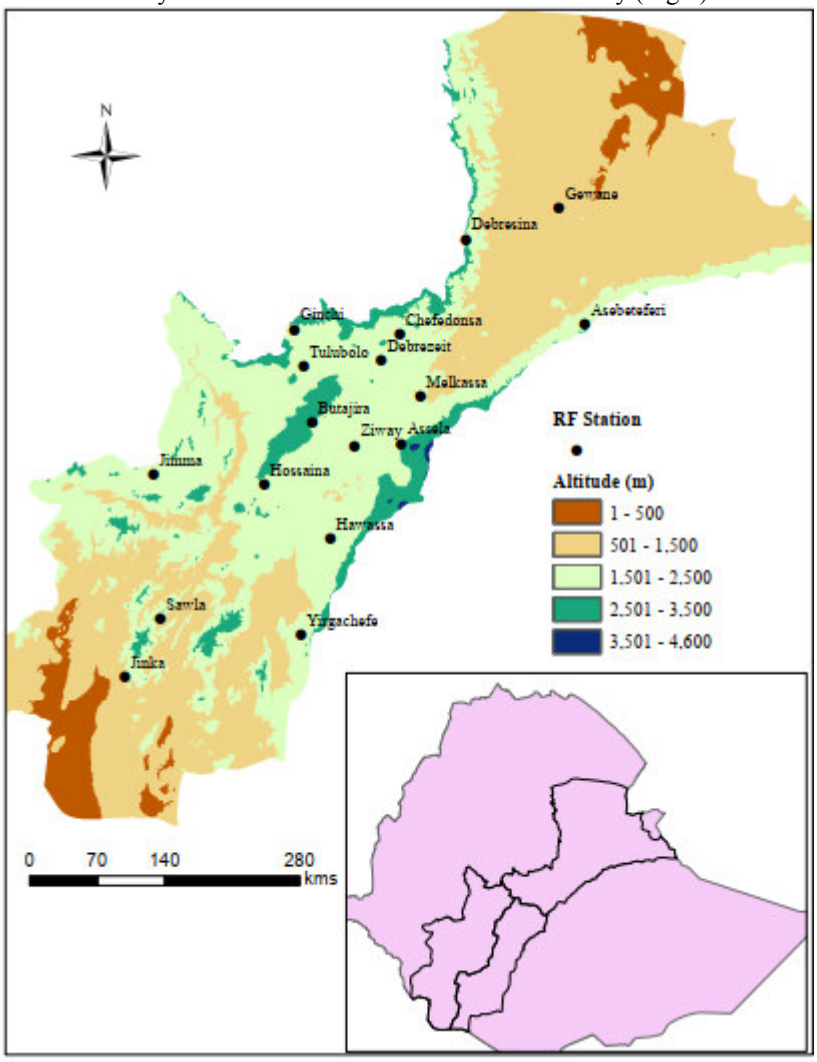

Fig 1. Altitudinal variations of the study area based on MoARD, 2005

The physiographic features of the GRVB are mainly the results of faulting and volcanism associated with rifting processes (Mechal et al., 2017). From a morphological and geological point of view, the region has been subdivided into three main segments: the northern, central, and southern (Wolde Gabriel et al., 1990; Abbate et al., 2015). The northern rift funnels from the Afar depression, where it is about 100 km wide, to the 80-km long

Dubeta Col sill (north of Ziway lake). The central rift, which is 80 km wide, includes most of the lake region and extends southward and has an average elevation of 1,600 m, and the lowest altitude is at Lake Abiyata (1,580 m). The southern Rift Valley narrows up to 60 km, shifts to a N–S trend, and reaches an elevation of 2,000 m, decreasing southward to 1,000 m (Abbate et al., 2015). The typical rift morphology is well developed and the three major physiographic regions, rift floor, escarpment and highland, are clearly visible (Mechal et al., 2017). The major tectonic scarp connects the rift floor with the uplifted plateau; the plateau rises to elevations of 3,200 m a.s.l., whereas the rift floor descends to 1,175 m a.s.l at Lake Abaya (Mechal et al., 2017).

The GRVB receive annual total rainfall ranging from about 160 mm at some locations of lower Awash to more than 1900 mm in the north central areas of Omo-Gibe basin. Similarly, the mean annual temperature also varies from 10 ˚C at higher altitudes of parts of the Rift Valley Lakes Basin to higher than 29 ˚C in the lowlands of the study area. The short rain (*Bulg*) is caused by humid easterly and south westerly winds from the Indian ocean, and main season (*Kiremt*), Autumn and Spring rains as a result of convergence in the low-pressure systems associated with the Inter Tropical Convergence Zone (Seleshi and Zanke, 2004). The climate of the basins varies as a function of the altitude, angle of the sun, distance from oceans, terrain and other factors such as influence of inter-tropical convergence zone (MoW&E, 2010).

2.2 Climate data sources

Daily measured weather data of 16 representative stations for the present climate (1981-2010), hereafter referred to as baseline, were obtained from the National Meteorological Agency of Ethiopia (http://www.ethiomet.gov.et). The stations have long years of relatively complete and quality records for at least 20 and more years. The selection ensured balanced representation of the major agroecology with data records of no more than 10% missing value (Seleshi and Zanke, 2004). Data quality have been ensured and published in Ademe et al. (2020). Projected changes in rainfall and temperature were analyzed based on 8 combinations of 4 Global Climate Model (GCMs) (CNRM-CM5, EC-EARTH, HadGEM2-ES and MPI-ESM-LR), dynamically downscaled by 1 Regional Climate Models (RCM) (RCA4) and 2 Representative Concentration Pathways (RCPs) (RCP4.5 and RCP8.5). High resolution dynamically downscaled projected climate data gridded over 0.5˚ X 0.5˚ of corresponding stations were used for the analysis. The projected data were obtained from Coordinated Regional Downscaling Experiment (CORDEX) for Africa dataset (http://www.cordex.org). The description of the climate models used in the study is shown in Table 1.

Table 1. Description of Global Climate Models (GCMs) and Regional Climate Models (RCMs) in the CORDEX-Africa GCM-RCM combinations used in this Study

Model	Short Name	Institution	Reference
GCM Models			
CNRM CERFACS CNRM-CM5	CNRM-CM5	Centre National de Recherches Météorologiques, France	(Voldoire et al., 2013)
EC-EARTH v2	EC-EARTH	EC-Earth Consortium, Europe	(Hazeleger, 2012)
MOHC HadGEM2-ES	HadGEM2-ES	Hadley Met Office Hadley Centre, UK	(Collins, W., 2011)
MPI MPI-ESM-LR	MPI-ESM-LR	Max Planck Institute for Meteorology (MPI-M)	(Giorgetta et al., 2013)
RCM models			
CCLM4.8 CCLM4.8	CLMcom	Climate Limited-Area Modelling Community (www.clm-community.eu)	(Rockel et al., 2008)
SMHI RCA4	RCA4	Sveriges Meteorologiska och Hydrologiska Institut, Sweden	(Samuelsson et al., 2015)

2.3 Climate change scenarios and downscaling

The study used two of the four RCPs: RCP4.5 (a relatively modest increase in greenhouse gas concentrations) and RCP8.5 (a rapid increase in greenhouse gas concentrations). RCP4.5 refers to a pathway in which the radiative forcing of greenhouse gases reaches 4.5W/m^2 in the year 2100 relative to pre-industrial levels, while RCP8.5 describes a pathway in which radiative forcing reaches 8.5 W/m^2 in the year 2100, relative to the pre-industrial levels (van Vuuren et al., 2011). Daily precipitation and temperature simulations under RCP4.5 and RCP8.5 scenarios were used to project future climate of the study basins.

Climate scenarios were generated by changing the baseline climate data based on outputs from GCM-RCMs/RCPs using the "Delta method" (Wilby et al., 2004). With the delta method, changes in rainfall were created by multiplying the rainfall scenario change factors with the baseline (1981-2010) daily values (1), while changes in minimum and maximum daily temperature are obtained by adding the temperature change factors to the baseline daily values (2) (Seaby et al., 2013). Consequently, a projected change in daily rainfall and mean daily temperature

from the eight GCM-RCM pairings and two RCPs by near, mid and end centuries were generated for analysis for each station considered in the study.

$$P_{\Delta}(i,j) = \Delta_p(j) * P_{obs}(i,j) \quad ; \quad \Delta_p(j) = \frac{\overline{P}_{fut}}{\overline{P}_{bas}} \tag{1}$$

$$T_{\Delta}(i,j) = \Delta_T(j) + T_{obs}(i,j) \quad ; \quad \Delta_T(j) = \overline{T}_{fut} - \overline{T}_{bas} \tag{2}$$

where P_{Δ}, and T_{Δ} are delta change perturbed daily climate change variables, P_{obs} and T_{obs} are observed climate variables in the baseline period, Δ_P and Δ_T are the changes in climate as simulated by the RCMs, $\overline{P}$ and $\overline{T}$ are daily climate means by annual basis, the index 'bas' and 'fut' indicates the baseline and future period, respectively.

2.4 Data analysis

2.4.1 Climate variability analysis

Coefficient of Variation (CV) and standardized anomaly index (SAI) were used as descriptors of rainfall variability and the nature of the trend. The descriptor has been widely used in many rainfall variability studies in Ethiopia and elsewhere (example: Bewket and Conway, 2007; Kassie et al., 2015; Bekele et al., 2016; Ademe et al., 2020). Station based analysis was undertaken to investigate the variability class for annual, main and short season rainfall. The stations were then regrouped based on the variability class after Hare (1983). According to Hare (1983), coefficient of variation (CV) of stations are classified as low for below 20% CV, high for CV in the range of 20-30% and CV values of more than 30% are regarded as very high variability. The coefficient of variation measures the overall variability of the rainfall in the area of interest. A higher value of CV indicates a rainfall greater variability and vice versa. It was computed using the formula:

$$CV = \frac{\sigma}{\overline{X}} \times 100 \tag{3}$$

where CV is the coefficient of variation; X-bar is the average long-term rainfall and σ is the standard deviation of rainfall

Standardized anomaly index (SAI) of rainfall has been calculated to examine the nature of the trends. It enabled the determination of the dry and wet years in the record and is used to assess frequency and severity of droughts and it is computed as:

$$SAI = \frac{Xi - \overline{X}}{\sigma} \tag{4}$$

where Xi is the annual rainfall of the particular year; X-bar is the long-term mean annual rainfall over a period of observation and σ is the standard deviation of annual rainfall over the period of observation. Negative values indicate a drought period as compared to the chosen reference period while the positive ones indicate a wet situation. The category of SAI values is indicated in the Table 2.

Table 2. Standardize anomaly index classification ((McKee et al., 1993)

SAI value	Category
Above 2	Extremely wet
1.5 to 1.99	Very wet
1.0 to 1.49	Moderately wet
-0.99 to 0.99	Near normal
-1.0 to -1.49	Moderately dry
-1.5 to -1.99	Severely dry
-2 or less	Extremely dry

2.4.2 Projected changes in rainfall and temperature

Delta changes in mean daily rainfall and daily temperature were computed for near, mid and far century climate relative to the baseline using the generated climate data of the climate models. Percent changes were calculated for all agroclimatic indices using (5). Annual and seasonal changes were considered using 30 years of simulated data for each station considered in the study. Delta changes in annual total rainfall and annual mean daily temperature were mapped to show spatial variations in the study areas.

$$\% \Delta = \frac{\text{Proj-Baseline}}{\text{Baseline}} X\ 100\% \tag{5}$$

where, Proj = projected value; Baseline = Baseline value; Δ= change

3. Results and Discussions

3.1 Spatial variations of annual and seasonal precipitation in the GRVB

Spatial variations in annual and seasonal rainfall amount received are portrayed in Fig 2. Across the study area, two distinct patterns of rainfall were depicted. The first pattern includes areas with bimodal rainfall where *Bulg* and *Kiremt* seasons prevail. In these areas, the short rainy season, *Bulg*, peaks in April, while the long rainy season, *Kiremt*, peaks in July. In some other areas, bimodal rainfall pattern in which the highest rainfall is received in the months of April (long season) and October (short season) was identified. The second pattern recognized in the study area is the monomodal pattern of rainfall with a long *Kiremt* season that stretches from March through November (Ademe et al., 2020). The basins receive a total annual rainfall ranging from 538 mm in the northern lowlands of the Awash basin to as high as 1494 mm in south and southwestern parts of the basin. Similarly, the main season rainfall of the basins ranges from 228 mm in the northern regions of the basin to 1226 mm in the southwestern monomodal rainfall region of the basins. These variations in the study basins may be explained by the geographical position of stations with respect to the equator. Mutai and Ward (2000) for example, discussed spring is the major rainfall period for the near-equatorial regions of extreme southern and southeastern Ethiopia which is associated with the long rainy season of equatorial East Africa whereas the northern and northeastern stations of which receive its monsoon rain start during May and June because of the ITCZ position during that period of time.

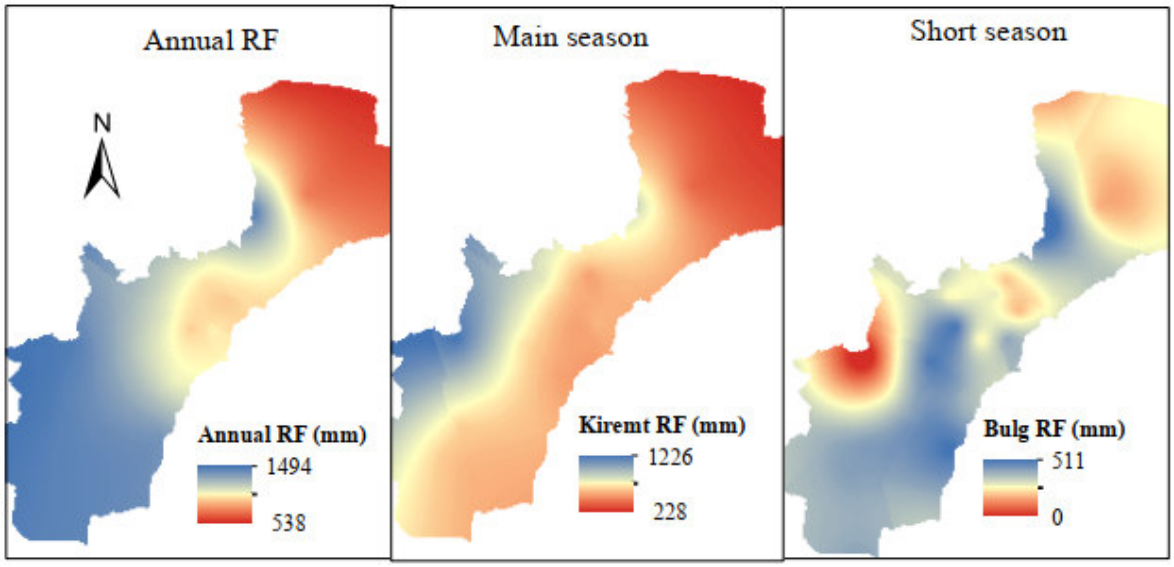

Fig 2. Spatial variations of annual and seasonal rainfall amount received by the Great Rift Valley Basins of Ethiopia

3.2 Spatial variations in rainfall variability across the GRVB

The rainfall of the study basins showed both spatial and temporal variabilities (Fig 3). The total annual rainfall of the basins showed variation in the year-to-year variability ranging from low at the southern half to high in the northern half of the study basins. The southern half of the study area (mainly Omo-Gibe and Rift Valley Lake Basins) which are nearer to the equator showed low rainfall variability while the northern part of the basin (Awash Basin) showed high annual variability. Similarly, seasonal variations in rainfall showed high to a very high variations in the majority of the study area. The central and southern parts of the basins showed high degree of variation while the northern part of the basin the main season rainfall showed a high to very high yearly variations that are challenging pertaining to agricultural planning and decision making. The short season however was very unsuitable to rainfed farming as the very high variation in rainfall and the amount received by the same was very low.

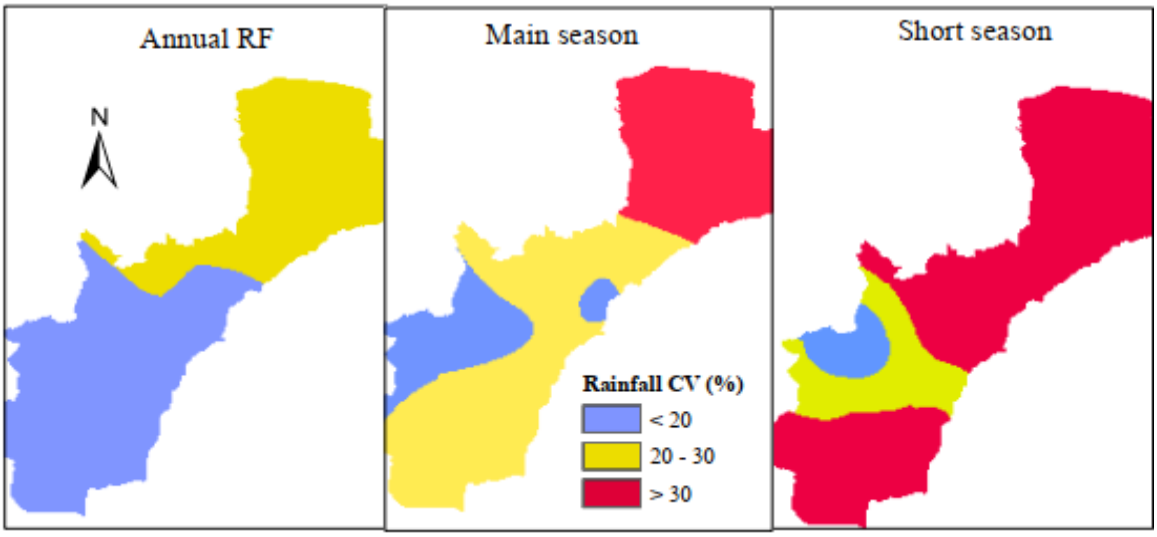

Fig 3. Spatial map of Rainfall variability class as expressed in coefficient of variation (%) across the Great Rift Valley Basins of Ethiopia

Similar results were published by Kassie et al. (2013), Gebremichael et al. (2014) and Bekele et al. (2016) for CRV in South Ethiopia and Awash Basin, respectively. The authors indicated a high coefficient of variation (CV% >30) for *Bulg* season rainfall than its corresponding *Kiremt* season. Seleshi and Zanke (2004) emphasized the causes of total and seasonal inter-annual variability of precipitation over Ethiopia. They indicated the forward and retreat pace of the African sector of the intertropical convergence zone (ITCZ) and their ending and beginning times vary annually, causing most of the inter-annual variability in rainfall over Ethiopia. The migration of ITCZ is sensitive to variations in Indian Ocean sea surface temperatures that vary from year to year, influencing the characteristics of the season in the region as well as episodes of El Niño Southern Oscillation and La Niña (Dessu and Melesse, 2013).

3.3 Standardized Anomaly Index of the GRVB

The percent dry, normal and wet years anomaly of the baseline period was calculated and map was generated for the GRVB as shown in Fig 4. Based on the index calculated, the majority of the annual rainfall of the basins fall under normal years of about 60% of the year in the southern half and 83% of the year for the northern half of the basins. It was shown that 10-20% of the years at southern and northern half of the basin respectively, receive above average rainfall with respect to the long-term average rainfall of the specific areas. Looking at the normal and wet years anomaly of the basins, the majority of the year seems favorable to rainfed farming given that the in-season distribution is quite favorable. The southern half of the study basins however, receive below average annual rainfall and exhibit moderate to extreme dryness. Spatially, the southern half of the basins receive annual total rainfall below the average in every 1 year out of 4 years period. The northern half of the basins however gets dry every 1 out of 17 years. Looking at the frequency of dry, normal and wet year occurrences in the study area, one can infer that the dry year was more frequently observed during the baseline period than the wet years signaling further pressure for rainfed farming under the warming future scenario in the basins.

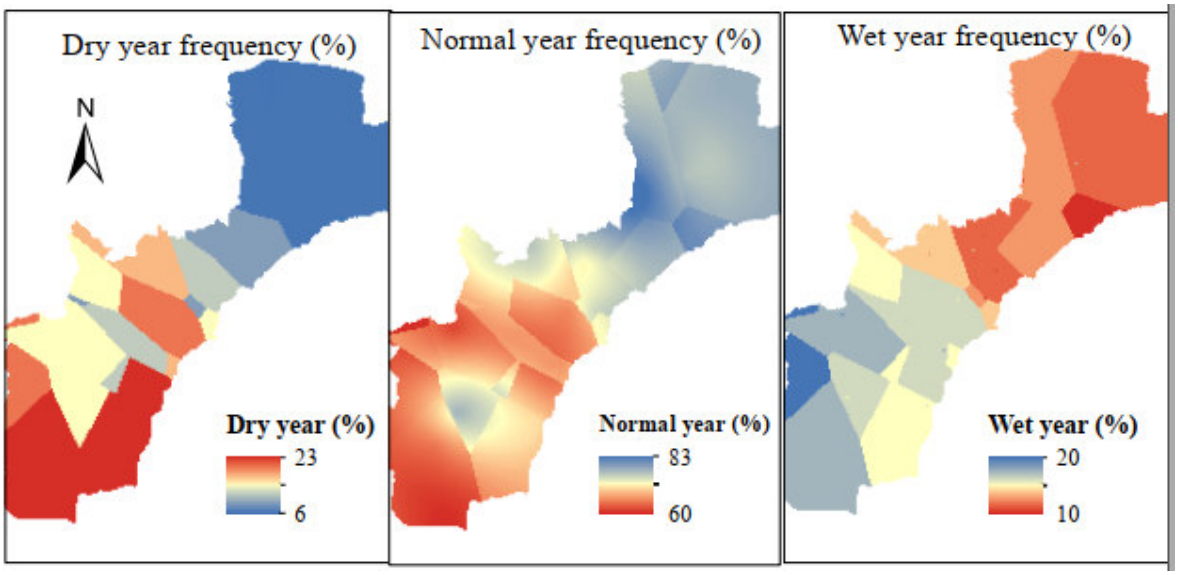

Fig 4. Spatial variation in percent of dry, normal and wet year in the GRVB of Ethiopia, 1981-2010.

Projected changes of rainfall in the GRVB

Projections based on eight combinations, i.e., eight GCM-RCM combinations, with two RCP scenarios suggested that the annual and seasonal rainfall showed variations in rainfall projection across the GRVB. Majority of the climate models however projected a decline in annual precipitation in the near, mid and end century for most of the stations in the GRVB relative to the baseline (1981-2010) (Fig 5). HaDGEM2-ES_RCA4 based projections for example, revealed changes in precipitation ranging from +4.2 to -16% and +3.8 to -18% for near period under RCP4.5 and RCP8.5 emission scenario, respectively. The near future projections indicated a likely decline in rainfall for the majority of stations by RCP4.5 as compared to RCP8.5 climate scenario. The mid and end century simulations however showed a highly likely decline in rainfall for the majority of stations under both RCPs except for Sawla and Jinka (Semi-arid locations in the southern part of the GRVB) where a likely increases in rainfall were simulated. Looking at the changes in the selected three stations representing the major three agroecologies in the GRVB suggest, highest declines in rainfall were simulated for the central semi-arid (Melkassa) areas followed by a considerable decline in the sub-humid (Assela) parts of the GRVB. The humid (Jimma) however showed a slight decline in rainfall across all periods and RCPs.

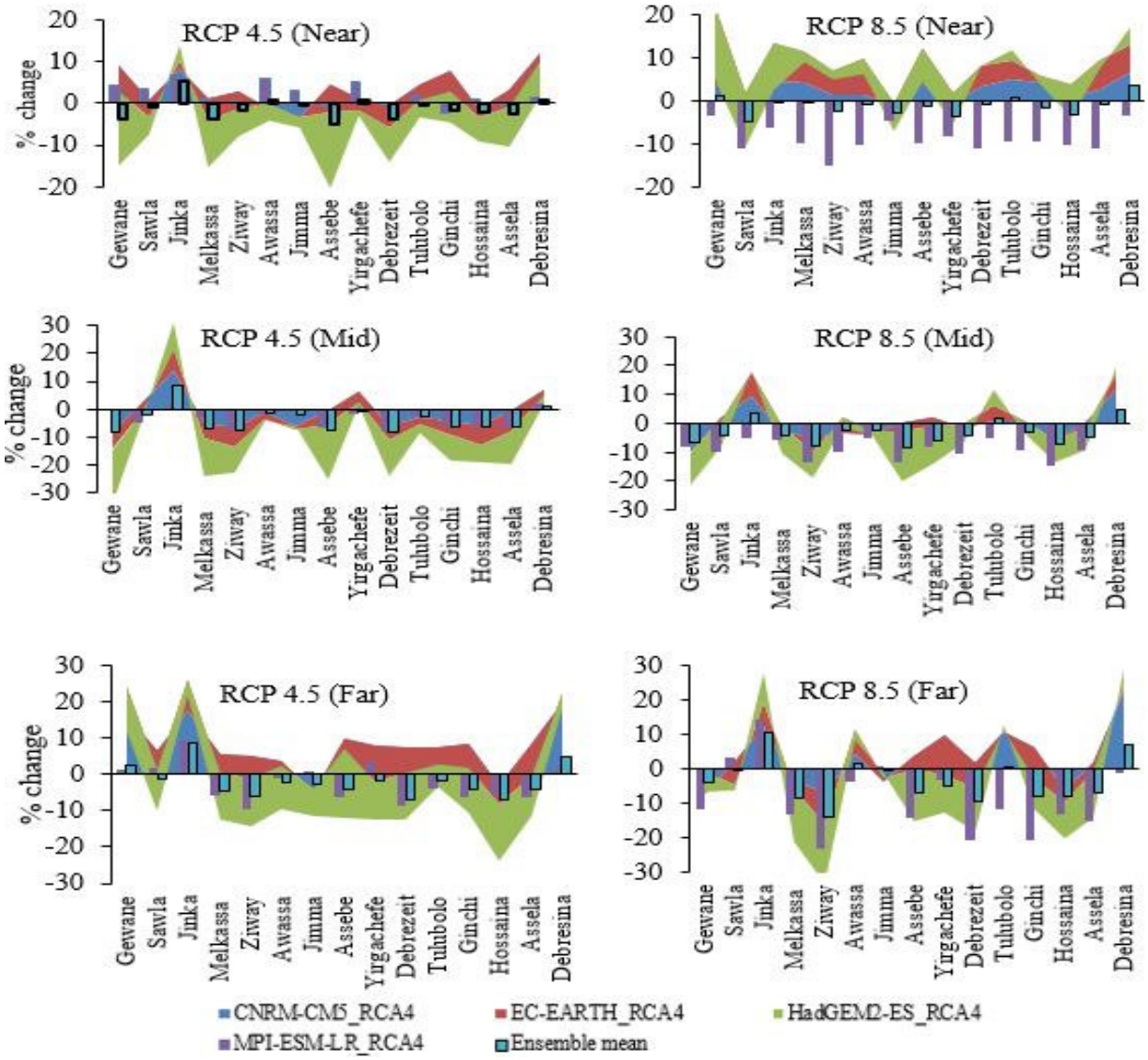

Fig 5. Changes in annual rainfall as projected by different climate models in near, mid and end century relative to the base period (1981-2010)

The change in annual rainfall simulations suggest a 6% increase from a single model and RCP (CNRM/RCP4.5) while the rest models and emission scenarios projected a change that range from -2% (by ECEARTH/RCP8.5) to -24% (by HadGEM2-ES/RCP8.5). The ensemble means of the model's projections over the basins indicated a likely decline in rainfall across all periods and emission scenarios indicating enormous pressure in the availability of soil moisture in the future period which could negatively affect rainfed crop production in the region. Reports suggest that such declines in rainfall during the past periods has costed Ethiopia millions of its peoples' lives. Studies indicated that a decline in 10% of seasonal rainfall from the long-term average translates to 4.4% decrease in the countries food production (von Braun, 1991). Projected decline in rainfall in the GRVB might signal serious food shortage and insecurity in the future periods unless proper adaptation measure is in place. Projection of future rainfall suggested that both annual and main season rainfall are most likely to decrease for most of the stations and climate scenarios. Our result agrees with past research findings on future rainfall projections for Ethiopia (Arndt et al., 2011; Kassie et al., 2015). A decrease of *Kiremt* rainfall by 4 to 20% for the central rift valley was reported during the mid-period under RCP4.5 and RCP8.5 emission scenario with respect to 1980-2009 period (Kassie et al., 2015). Similar result was also reported by Arndt et al. (2011) indicating that the *Kiremt* rainfall will decline by 20% and the *Bulg* rainfall will decline by 5-6% by 2080s relative to the 1960-1990 period.

Projected changes of temperature in the GRVB

Unlike precipitation, the entire basin may experience increases in temperature in the near mid and end century as

compared to the baseline (Table 3). Almost all the considered models projected an increase in temperature consistently across the stations and periods. Under each future period, higher positive changes were projected for all stations under RCP8.5 than the corresponding RCP4.5 scenarios. The ensemble of models by RCP suggested Melkassa (semi-arid) might be warmer by 1.49 to 2.12 ºC while Assela (sub-moist) is projected to warm by 1.52 to 2.15 ºC in the near future relative to the baseline under RCP4.5 and RCP8.5, respectively. Similarly, projections suggest increases of 1.2 to 1.75 ºC for the humid parts of the basin (Jimma) by mid-century. On the other hand, GCM_RCM combinations differ in the magnitude of change under both RCP scenarios and periods, although they consistently projected increases in temperature across stations and periods. HadGEM2-ES_RCA4 model projected the highest increase across all periods for each location than the rest models while CNRM_RCA4 projected the least relative to the other models. The different models projected a wide range of temperature increases for the representative stations under each RCP. The projections at Melkassa for instance showed an increase from +0.65 ºC (by CNRM_RCA4) to +0.95 ºC (by HadGEM2-ES_RCA4) in the near period which will likely to further escalate during mid (1.38 to 1.76 ºC) and far (1.85 to 2.29 ºC) periods under RCP4.5 scenario. In similar token, the worst-case scenario (RCP8.5) was projected to increase Melkassa temperature in the range between +0.77 ºC (by ECEARTH_RCA4) to 1.09 ºC (by HadGEM2-ES_RCA4) in the near term and again will likely double in the mid (+ 1.89 to + 2.5 ºC) as well as by end (3.2 to 4.24 ºC) century using the same set of models. It was observed from the analysis that all agroecology will likely warm in the future but the change of temperature between two consecutive periods will be higher for the semi-arid lowlands (Melkassa) than that of the humid regions (Jimma) under both RCP scenarios.

Table 3. Changes in temperature (ºC) for near, mid and far periods for selected stations in the GRVB simulated by RCA4 based RCM under two IPCC RCP scenarios with respect to 1981-2010 baseline

	Near (2021-2040)			Mid (2041-2070)			End (2071-2100)		
GCM_RCM	Melkassa	Assela	Jimma	Melkassa	Assela	Jimma	Melkassa	Assela	Jimma
RCP4.5									
CNRM_RCA4	0.65	0.63	0.48	1.38	1.28	1.04	1.85	1.73	1.41
ECEARTH_RCA4	0.68	0.74	0.62	1.37	1.5	1.23	1.71	1.89	1.56
HadGEM2-ES_RCA4	0.92	0.95	0.7	1.76	1.8	1.32	2.29	2.34	1.79
MPI-ESM_RCA4	0.78	0.78	0.63	1.47	1.51	1.21	1.71	1.73	1.41
Ensemble mean	0.76	0.77	0.61	1.49	1.52	1.2	1.89	1.92	1.54
RCP8.5									
CNRM_RCA4	0.79	0.74	0.62	1.94	1.8	1.45	3.5	3.22	2.54
ECEARTH_RCA4	0.77	0.82	0.71	1.89	2.09	1.73	3.2	3.54	3.02
HadGEM2-ES_RCA4	1.09	1.12	0.9	2.5	2.53	1.95	4.24	4.29	3.32
MPI-ESM_RCA4	0.97	1	0.86	2.15	2.18	1.86	3.83	3.86	3.19
Ensemble mean	0.91	0.92	0.77	2.12	2.15	1.75	3.69	3.73	3.02

To understand the spatial variation of changes in temperature across the basins, HadGEM2-ES_RCA4 model results were mapped for the two RCP scenarios and the three future periods relative to the base period (Fig 6). Temperature is projected to rise from +0.7 to +1.25 ºC under RCP4.5 to +0.9 to +1.6 ºc under RCP8.5 across the basin in the near future. The temperature likely to escalate by mid and end century where in northeastern lowlands, the changes may likely rise up to +4 to +6 ºc. The modest RCP scenario projected an increase in temperature ranging from +2.6 (mid) to +3.4 ºC (end century) which could adversely affect agriculture and water resources and in-turn directly or indirectly affecting millions who dwell in the basins. In the future, all the models showed increases in temperature across all the stations considered in the study. The study suggested the warming trend will continue and the annual temperature is expected to increase in the range of 2.5-5.1 ºC averaged over RCPs by the end of this century.

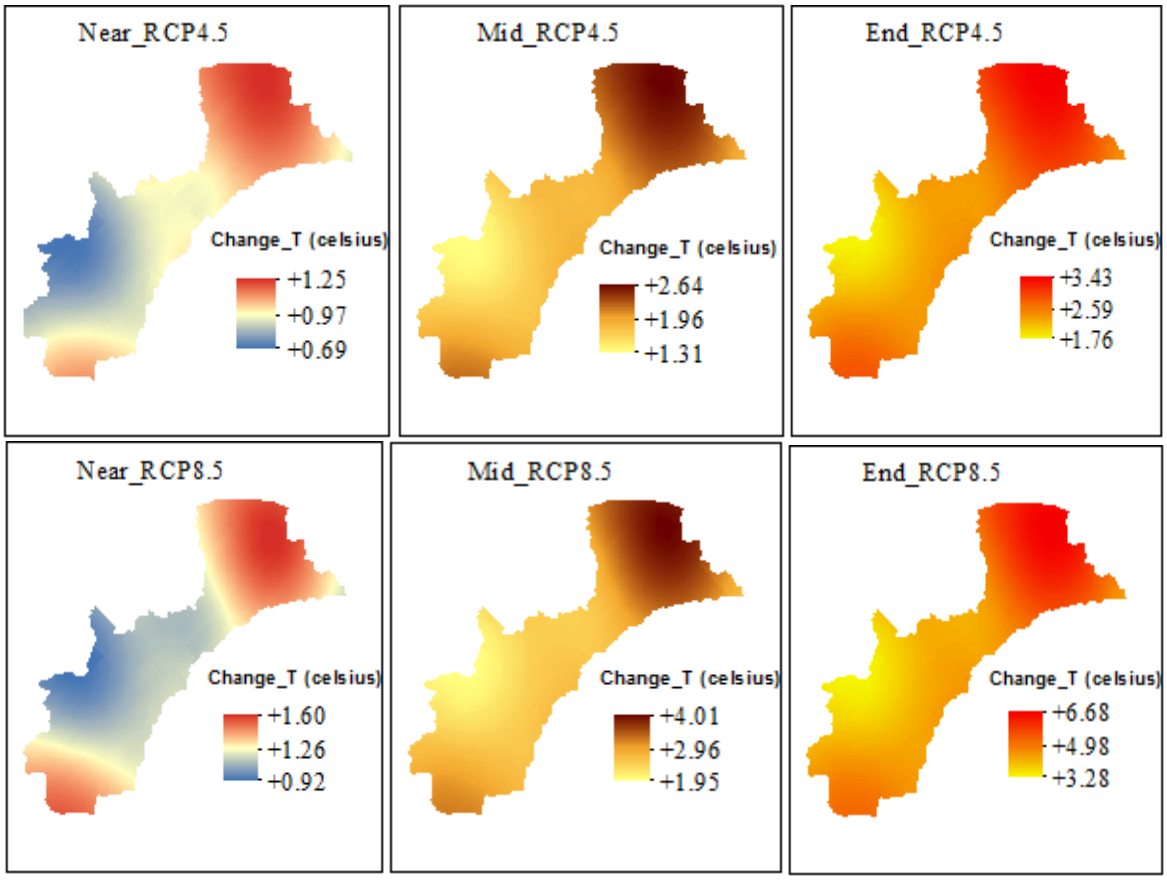

Fig 6. Changes in annual average temperature (ºC) as projected by HadGEM2-ES_RCA4 RCM in near, mid and end of century relative to the baseline (1981–2010).

The result of this study is consistent with reports of various global, regional and national scales. For global scale projection, the Fifth IPCC assessment synthesis report suggested an increasing trend of temperature in the range of 1.4 to 4.8 ºC by the end of the century under RCP4.5 and RCP8.5 concentration pathway (IPCC, 2014). Regional and sub regional warming was also indicated for East and Central Africa by about +2 ºC during 2050s (Kwena et al., 2018). Similarly, for Ethiopia, NMA (2007) reported that the annual temperature is expected to increase in the range of 2.7 to 3.4 ºC by the 2080s compared to the 1961-1990 baseline. The highest increases are indicated in the lowland areas which are currently characterized by extremely high temperature in the basin. These could signify that; the climate change is expected to worsen the situation in the currently hotter regions while the relatively warmer and cooler regions might suffer by unprecedented warming in the future.

Conclusion

Annual and seasonal rainfall variability, declining rainfall amount in the baseline and projected periods coupled with increasing temperature suggest a pressing challenge for rainfed crop production in the region. High frequency in dry years was observed during baseline period which critically affect rainfed production. The degree of risk however showed spatial variation across the basin and climate change scenario where arid and semiarid areas are being affected and might highly likely be further affected in the future. The increasing temperature on the other hand will increase the rate of evapotranspiration and crop water requirements, adding to the currently frequent water stress of crops in the relatively drier parts of the GRVB. Rainfed crop production in the region, which is already impacted by the current climate variability, is likely to be further challenged with future climate change. As a consequence, specific impact -based adaptation strategies are essential to reduce the vulnerability of rainfed crop production in the area.

Reference

Abbate, E., Bruni, P., Sagri, M., 2015. Geology of Ethiopia: A Review and Geomorphological Perspectives, in: Billi, P. (Ed.), Landscapes and Landforms of Ethiopia, World Geomorphological Landscapes. Springer Science+Business Media Dordrecht, pp. 33–64.

Ademe, F., Kibebew, K., Sheleme, B., Mezgebu, G., Gashaw, M., 2020. Rainfall analysis for rain-fed farming in the Great Rift Valley Basins of Ethiopia. J. Water Clim. Chang. 11, 812–828.

https://doi.org/10.2166/wcc.2019.242
Araya, A., Stroosnijder, L., 2011. Assessing drought risk and irrigation need in northern Ethiopia. Agric. For. Meteorol. 151, 425–436.
ARBWA, (Awash River Basin Water Audit Project), 2013. Coping with Water Scarcity, the Role of Agriculture. Developing a Water Audit for Awash River Basin. Synthesis report, GCP/INT/072/ITA. Addis Ababa, Ethiopia.
Arndt, C., Robinson, S., Willenbockel, D., 2011. Ethiopia's growth prospects in a changing climate: A stochastic general equilibrium approach. Glob. Environ. Chang. 21, 701-710.
Awulachew, S.B., Erkossa, T., Namara, R.E., 2010. Irrigation Potential in Ethiopia: Constraints and Opportunities for Enhancing the System. International Water Management Institute, Colombo, Sri Lanka.
Bekele, D., Alamirew, T., Kebede, A., Zeleke, G., Melese, A.M., 2016. Analysis of rainfall trend and variability for agricultural water management in Awash River Basin, Ethiopia 5, 127–141. https://doi.org/10.2166/wcc.2016.044
Bewket, W., Conway, D., 2007. A note on the temporal and spatial variability of rainfall in the drought-prone Amhara region of Ethiopia 1477, 1467–1477.
Collins, W., et al., 2011. Development and evaluation of an Earth-system model–HadGEM2. Geosci. Model Dev. 4, 1051–1075.
Conway, D., Schipper, E.L.F., 2011. Adaptation to climate change in Africa: Challenges and opportunities identified from Ethiopia. Glob. Environ. Chang. 21, 227–237.
Dessu, S.B., Melesse, A.M., 2013. Impact and uncertainties of climate change on the hydrology of the Mara river basin, Kenya/Tanzania. Hydrol. Process 27, 2973–2986.
ECRGE, (Ethiopia's Climate Resilient Green Economy), 2015. Agriculture and Forestry Climate Resilience Strategy. Ministry of Environment and Forest (MEF), Ministry of Agriculture (MoA), Addis Ababa, Ethiopia.
Gebremichael, A., Quraishi, S., Mamo, G., 2014. Analysis of Seasonal Rainfall Variability for Agricultural Water Resource Management in Southern Region, Ethiopia. J. Nat. Sci. Res. 4, 56–79.
Giorgetta, M.A., Jungclaus, J., Reick, C.H., Legutke, S., Bader, J., ..., Marotzke, J., Stevens, B., 2013. Climate and carbon cycle changes frm 1850 to 2100 in MPI-ESMsimulations for the Coupled Model Intercomparison Project phase 5. J. Adv. Model. Earth Syst. https://doi.org/10.1002/jame.20038
Hare, F.K., 1983. Climate and Desertification. Revised analysis (WMO-UNDP) WCP-44 pp 5-20. Geneva, Switzerland.
Hazeleger, et al., 2012. EC-Earth V2.2: Description and validation of a new seamless Earth system prediction model. Clim. Dyn. 39, 2611–2629.
IPCC, 2014. Climate Change 2014: Synthesis Report. Contribution of Working Groups I, II and III to the Fifth Assessment Report of the Intergovernmental Panel on Climate Change [Core Writing Team, R.K. Pachauri and L.A. Meyer (eds.)]. IPCC, Geneva, Switzerland 151 pp.
Kassie, B.T., Asseng, S., Rotter, R.P., Hengsdijk, H., Ruane, A.C., Van Ittersum, M.K., 2015. Exploring climate change impacts and adaptation options for maize production in the Central Rift Valley of Ethiopia using different climate change scenarios and crop models. Clim. Change 129, 145–158. https://doi.org/10.1007/s10584-014-1322-x
Kassie, B.T., Rötter, R.P., Hengsdijk, H., Asseng, S., Ittersum, V., K., M., Kahiluoto, H., Van Keulen, H., 2013. Climate variability and change in the Central Rift Valley of Ethiopia: challenges for rainfed crop production. J. Agric. Sci. 152, 58–74.
Kwena, K., Ademe, F., Serge, J., Asmerom, N., Musana, B., Razakamiarmanana, R., Ruttoh, R., Mogaka, H., Dereje, A., Woldearegay, K., Esilaba, A., Emongor, R., 2018. Bringing climate smart agriculture to scale: Experiences from the water productivity project in East and Central Africa, in: Shanker, A. (Ed.), Climate Resilient Agriculture.
McKee, T.B., Doesken, N.J., Kleist, J., 1993. The relationship of drought frequency and duration to time scales, in: In Eighth Conference on Applied Climatology, 17–22 January 1993. Anaheim, CA, USA.
Mechal, A., Birk, S., Dietzel, M., Leis, A., Winkler, G., Mogessie, A., Kebede, S., 2017. Groundwater flow dynamics in the complex aquifer system of Gidabo River Basin (Ethiopian Rift): a multi-proxy approach. Hydrogeol J 25, 519–538.
MoARD, 2005. Agro-ecological zonation of Ethiopia. Addis Ababa, Ethiopia. Addis Ababa, Ethiopia.
MoWE, 2010. Basin Description [WWW Document]. URL www.mowr.gov.et/index.php?pagenum=3.3&pagehgt=1000px (accessed 8.27.16).
Müller, C., Cramer, W., Hare, W.L., Lotze-Campen, H., 2011. Climate change risks for African agriculture. ,. Proc. Natl. Acad. Sci. 108, 4313–4315.
Mutai, C.C., Ward, M.., 2000. East African rinfall and the tropical circulation/convection on intraseasonal to interannual timescales. J. Clim. 13, 3915–3939.

NMA, 2007. Climate change national adaptation programme of action (NAPA) of Ethiopia:Technical Report, National Metorological Agency, Addis Abeba, pp. 85. Addis Abeba, Ethiopia.

NMA, 1996. Climatic and Agroclimatic Resources of Ethiopia. Vol. 1, No. 1. National Meteorology Agency, Addis Ababa, Ethiopia.

Rockel, B., Will, A., Hense, A., 2008. The Regional Climate Model COSMO-CLM (CCLM). Meteorol. Zeitschrift 17, 347–348.

Samuelsson, P., Golvick, S., Janssen, C., Kuplainen, M., Kourzeneva, E., van de Berg, W., 2015. The surface proccesses of the Rossby Center regional atmospheric climate model (RCA4). Meteorology Nr 157. SMHI, SE-601 76 Norrkoping, Sweden.

Seaby, L.P., Refsgaard, J.C., Sonnenborg, T.O., Stisen, S., Christensen, J.H., Jensen, K.H., 2013. Assessment of robustness and significance of climate change signals for an ensemble of distribution-based scaled climate projections. J. Hydrol. 486, 479–493. https://doi.org/10.1016/j.jhydrol.2013.02.015

Seleshi, Y., Zanke, U., 2004. Recent changes in rainfall and rainy days in Ethiopia 20, 973–983. https://doi.org/10.1002/joc.1052

Stern, N.H., 2007. The economics of climate change: the Stern review. Cambridge University Press, pp.673.

Thornton, P.K., Jones, P.G., Alagarswamy, G., Andresen, J., Herrero, M., 2010. Adapting to climate change: agricultural system and household impacts in East Africa. Agric. Syst. 103, 73–82.

Thornton, P.K., Jones, P.G., Ericksen, P.J., Challinor, A.J., 2011. Agriculture and food systems in Sub-Saharan Africa in a 4 oC+ world. Philosophical Transactions of the Royal Society A. Math. Phys. Eng. Sci. 369, 117–136.

UNDP, 2018. Ethiopia National Human Development Report 2018; Industrialization with a Human Face World Economic Forum, 2018. The Global Competitiveness Report. UNDP Ethiopia, Addis Ababa, Ethiopia.

van Vuuren, D.P., Edmonds, J., Kainuma, M., Riahi, K., Thomson, A., Hibbard, K., Hurtt, G.C., Kram, T., Krey, V., Lamarque, J.F., Masui, T., Meinshausen, M., Nakicenovic, N., Smith, S.J., Rose, S.K., 2011. The representative concentration pathways: An overview. Clim. Change 109, 5–31. https://doi.org/10.1007/s10584-011-0148-z

Voldoire, A., Sanchez-Gomez, E., Melia, D.S.Y., Decharme, B., Cassou, C., Senesi, S., Valcke, S., Al., E., 2013. The CNRM-CM5.1 global climate model: Description and basic evaluation . Clim. Dyn. 40, 2091–2121.

von Braun, J., 1991. A policy agenda for famine prevention in Africa. Food policy statement No. 13. IFPRI, Washington DC. Washington DC, USA.

Wilby, R.L., Charles, S.P., Zorita, E., Timbal, B., Whetton, P., Mearns, L.O., 2004. Guidelines forUse of Climate Scenarios Developed fromStatistical Downscaling Methods 1–27. https://doi.org/citeulike-article-id:8861447

Wolde Gabriel, G., Aronson, J.L., Walter, R.C., 1990. Geology geochronology and rift basin development in the central sector of the Main Ethiopian Rift. Geol Soc Am Bull 102, 439–458.

World Bank, 2006. Managing water resources to maximize sustainable growth: A country water resources assistance strategy for Ethiopia. World Bank, Washington, DC. Washington, DC.